



## APPLICATION OF THE DISPERSION ENTROPY WITH SLIDING WINDOW FOR THE ANALYSIS OF MECHANICAL SYSTEMS

Jędrzej BLAUT<sup>1,\*</sup> , Łukasz BREŃKACZ<sup>1,2</sup> 

<sup>1</sup> AGH University of Krakow. Poland

<sup>2</sup> Institute of Fluid Flow Machinery, Polish Academy of Sciences. Gdańsk, Poland

\* Corresponding author, e-mail: [blaut@agh.edu.pl](mailto:blaut@agh.edu.pl)

### Abstract

This paper presents the possibility of using the dispersion entropy with a sliding window to assess the stability of machine operation. Attention was focused on the feasibility of using a sliding window and the assessment of the minimum length of the window that produces stable results. The answer to this question is open to all and depends on the complexity of the physics of the phenomenon. The research was carried out first for simple mechanical systems, then for non-linear systems, and then, in the final part of the research, attention was paid to the real signals describing the displacement of the pan in the bearing. These studies are important in determining the minimum window length to conclude the diagnosis of mechanical systems; the narrower the window, not only reduces the need for computing power but above all allows a faster response.

Keywords: dispersion entropy, sliding window, stability assessment, machine operation, mechanical systems, nonlinear systems, real signals, bearing displacement

## 1. INTRODUCTION

Diagnostics, as a field of engineering science and practice, has its roots dating back to the early twentieth century, when industrial development required more advanced methods of managing and maintaining machinery and infrastructure. Diagnostics encompasses methods and techniques to identify, locate, and characterise faults or anomalies in technical systems, which is the key to ensuring their safety and operational efficiency [1].

The first systematic approaches to diagnostics date back to the 1930s when the growth of the aerospace and automotive industries necessitated the creation of methods to assess the condition of machinery. Initially, these were simple visual and manual techniques, which evolved into advanced measurement methods [2].

Diagnostics has found its way into virtually every field of technology - from automation to energy to medicine. In automation and robotics, it is used to monitor the condition of machines and prevent failures. In power engineering, it allows the continuity of the energy supply to be maintained through the early detection of faults in the network and components of the power plant. In medicine, diagnostics is about identifying diseases and assessing the health of patients, using a variety of imaging and biological analysis techniques [3, 4].

Developments in technology, particularly in the area of sensors and measurement systems, have contributed significantly to advances in diagnostics. Methods such as thermography, ultrasound, vibration analysis, or techniques based on sensor data have become industry standards. Modern approaches such as big data analysis and machine learning are opening up new perspectives for automated real-time diagnostics [5].

The article [6] presents an overview of diagnostic methods that use genetic algorithms to analyse degradation processes in power units that work with renewable energy sources. The paper pays particular attention to the use of genetic algorithms for thermos fluid diagnostics of steam turbines, which are controlled by a central power system to stabilise renewable sources. Diagnostic procedures developed in the research facilitate the formation of a reverse model for the thermal power plant. This enables quick identification of general extremes by aligning simulated signals with indicators of degradation.

Progress in diagnostics relies on the advancement of the miniaturisation of measurement devices, their seamless integration with the Internet of Things, and the enhancement of intelligent algorithms for predictive maintenance of machinery and equipment. The development of these technologies is expected to contribute to even greater

efficiency and cost reduction in the operation of technical equipment [7].

Research into new methods of technical diagnostics is focused on extending the service life of equipment. To this end, new hardware solutions are being developed, e.g. high-precision fault-tolerant sensors. At the same time, advanced signal processing techniques are being developed to meet the new objectives. Currently, special attention is being paid to the non-linear analysis of diagnostic signals.

The analysis of operating parameters makes it possible not only to assess the current state of machines, but also to predict their future states. The basic premise of diagnostics is the postulate linking the increase in vibroacoustic energy levels with the progression of the degradation process. Therefore, it is necessary to develop advanced diagnostic methods that accurately identify the boundary between the normal state and the point at which it becomes unsafe to continue operating the equipment.

Although numerous machines can be characterised by linear models, nonlinear distortions often manifest in their operation, necessitating the use of nonlinear models for accurate description. Variations in machine behaviour may arise from factors such as wear and tear or the inherent instability of their operation. Many objects, including hydrodynamic bearings in specific operating states, do not get an adequate description by linear models. Despite extensive research conducted in scientific centres, the intricate physical phenomena of hydrodynamic bearings persistently fascinated researchers [8]. The mathematical models for hydrodynamic bearings enable for a precise prediction of their behaviour, although requiring the consideration of numerous parameters. Developing these parameters and conducting simulations typically consume significant time. Given the array of bearing designs, there is a pressing need to develop new, more accurate models [9].

### 1.1 Bearing diagnostics

Bearing diagnostics constitutes a crucial aspect of machine maintenance and condition monitoring. Bearings serve as vital components in most rotating machinery, and their malfunction can result in severe failures and subsequent downtime. Efforts to develop diagnostic methods within this domain prioritise early detection of problems, facilitate proactive maintenance planning, and prevent costly repairs [10].

Conventional approaches to bearing diagnosis rely on vibration analysis. Using advanced signal processing algorithms such as Fast Fourier Transform (FFT) and entropy-based techniques, it becomes feasible to precisely identify alterations in vibration signals, potentially indicating issues such as pitting, delamination, or lubrication disorders [11].

In article [12], the authors outline a methodology to determine the dynamic coefficients of the

bearings. The dynamic coefficients of the two hydrodynamic bearings were determined through experimental investigations. A methodology was developed, using impulse response analysis, to calculate stiffness, damping, and mass coefficients. This unified algorithm accommodated varying rotational speeds for a complete analysis. Tests were carried out with a modal hammer and shaft displacements were measured using eddy current sensors [13]. The experiments took into account the influence of a variety of parameters on the results obtained [14], which allowed a more complete description of the dynamic state of the rotors. Analysis has shown that the method can effectively identify differences in bearing behaviour at different loads and speeds, providing valuable information for diagnostic and maintenance activities [15].

Other approaches, based on STFT (Short-Time Fourier Transform) or wavelet analysis methods, are used for more specialised investigation of bearing characteristics. They allow the types of damage to be distinguished according to their unique frequency characteristics [16].

Recent research has focused on applying deep learning and its methods to automate bearing diagnostics. These techniques, using large data sets and the ability to 'learn' diagnostic features autonomously, enable the creation of predictive systems that can predict the time to bearing failure with high precision [17].

In an article [18] Blaut and Breńkacz analysed the effect of rotor imbalance on the value of the Teager-Kaiser energy operator (TKEO) in hydrodynamic bearings. The analysis employs TKEO, a method of calculating the rapid energy calculation method previously used in diagnostics, such as assessing hydrodynamic bearing instability and detecting gearbox failures. The study details the application of the Teager-Kaiser method to evaluate rotor imbalance in hydrodynamic bearings, conducted through an experimental investigation of the impact of rotor imbalance on the energy operator value. The experimental results confirm the usefulness of TKEO in machine condition assessment, demonstrating a clear correlation between changes in operating parameters and TKEO values, which contributes to a better understanding of rotor dynamics and its impact on machine operations.

### 1.2 Dispersion entropy

Dispersion entropy (DisEn), based on Shannon entropy, is a tool that allows the rapid determination of signal irregularities. The concept of symbolic dynamics originates from the simplification of measurements, in which the time series transforms a new signal comprising only a limited set of distinct elements. The analysis of the signal dynamics is based on the analysis of a sequence of symbols, which may lead to the loss of some detailed information but at the same time makes it possible to

preserve the invariant, robust features of the dynamics.

The best known methods based on symbol entropy are approximate entropy permutation entropy and DisEn, as used in this work. DisEn represents an innovative approach to monitoring unbalanced temporal signals. In the context of the analysis of one-dimensional signals, of length  $N$ , represented by the time series  $x = \{x_1, x_2, \dots, x_N\}$

Simplifying signal analysis using the dispersion entropy (DisEn) method consists of four main steps (fig. 1):

Step 1: assign signal elements to classes using different linear and non-linear approaches. This allows for efficient classification of the signal elements.

Step 2: Identify possible dispersion patterns by creating embedding vectors, where each vector has a specific embedding length and time delay. These vectors form the dispersion patterns that are used for further analysis.

Step 3: Count the incidence of each potential dispersion pattern by calculating the relative frequencies.

Step 4: Calculation of entropy based on Shannon's definition of entropy. The resulting entropy value, DisEn, reflects the degree of chaotic and unpredictable nature of the signal, taking into account the dimension of the embedding, the time delay, and the number of classes.

In this way, the DisEn method makes it possible to analyse and evaluate the degree of signal chaos, which can be useful for monitoring vibration signals in machine diagnostics. A comprehensive mathematical description can be found in the work of Rostaghi [19].

The normalised dispersion entropy can be written as

$$NDisEn(x, m, c, d) = \frac{DisEn(x, m, c, d)}{\ln(c^m)} \quad (1)$$

where  $m$  is the dimension of the embedding,  $c$  is the number of classes, and  $d$  is the time delay.

When determining the entropy, it is necessary to choose the appropriate parameter values. In the case of DisEn, there are three parameters: the embedding dimension  $m$ , the number of classes  $c$  and the time delay  $d$ . In this paper, the parameters determined by Rostaghi are adopted [20]. It analysed the effect of the parameters on the vibration signal of a properly

functioning bearing from the Case Western Bearing Dataset [21]. When the embedding dimension  $m$  is large, the DisEn algorithm may struggle to detect small changes effectively. Theoretically, if  $c$  is too small, two widely separated amplitude values can be assigned to a similar class, whereas a large value of  $c$  can lead to even a slight change altering their class, rendering the DisEn method sensitive to noise. Additionally, a high value of  $c$  can negatively impact the computation time. Furthermore, increasing the time delay  $d$  beyond the value of  $d = 4$  leads to an increase in the DisEn standard deviation of the signals.

### 1.3 Use of disentropy in diagnostics

Entropy, as a measure of the uncertainty or randomness of a system, is a fundamental concept in information theory, statistics, physics, and increasingly in diagnostic engineering. In 1948, Shannon defined information entropy, which became the basis for many subsequent theories and applications in various fields of science and technology [22]. Since then, different variations of entropy have been adapted to specific applications, including approximation entropy (ApEn) as a measure of the complexity of biological and financial systems introduced by Pincus in 1991 [4], and permutation entropy (PE), which was proposed by Bandt and Pompe in 2002 as a tool to study the complexity of time series data [23].

These methods have served as a basis for further research and the development of new concepts such as dispersion entropy (DisEn). Dispersion entropy, introduced by Rostaghi and Haddadnia in 2016, is one of the most recent extensions in this field [19]. DisEn is used to analyse the complexity of signals by assessing their dynamics and unpredictability. In the context of machine diagnostics, DisEn has proven particularly useful due to its ability to detect subtle irregularities and instabilities in signal data.

In the context of mechanical engineering, the size of the time window is crucial to the accuracy and effectiveness of the dispersion entropy as a diagnostic method. Work such as that by Hamed Azami and Mohsen Rostaghi (2016) introduces dispersion entropy as a method of temporal analysis, highlighting the importance of appropriate selection of time windows to preserve signal dynamics [19].

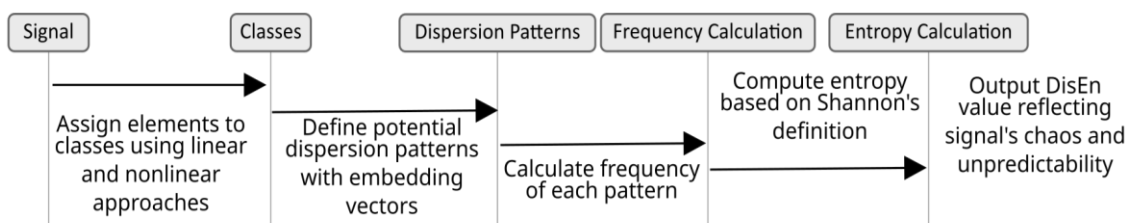


Fig. 1. Diagram of the dispersion entropy (DisEn) method

An article by Sandoval et al. [24] presents a study using entropy-based indicators to diagnose bearing failure. The study focusses on the importance of monitoring bearing conditions in wind turbines, where low operating speeds and high loads make it difficult to use traditional vibration techniques. The paper introduces new techniques, such as approximation entropy, dispersion entropy, singular value decomposition entropy, spectral entropy, and permutation entropy, which increase the effectiveness of vibration analysis in bearing condition diagnosis. They were used to analyse vibration signals obtained on a purpose-built test platform with bearings of different operating conditions. The results show that entropy-based indicators can distinguish damaged bearings at low speeds with greater accuracy compared to traditional indicators. Furthermore, the integration of traditional and entropy-based indicators improves the reliability of diagnosis.

## 2. SIMULATION STUDIES

To demonstrate the use of DisEn with a sliding window, numerical experiments were carried out on signals that describe basic mechanical systems. The work started for the simplest mechanical cases, and then the model was extended. The displacement and total energy diagrams of the systems are shown for easier interpretation. Another solution would be to add displacement, velocity, or acceleration diagrams.

### 2.1 Natural vibrations of a system with one degree of freedom

When examining a system with one degree of freedom, governed by the equation of motion,

$$m\ddot{x} + kx = 0, \quad (2)$$

we obtain the solution

$$x = A \cos(\omega t + \varphi) \quad (3)$$

and DisEn determined from the displacement. Figure 2 illustrates the displacement-time plot for the system as described by Equation (2).

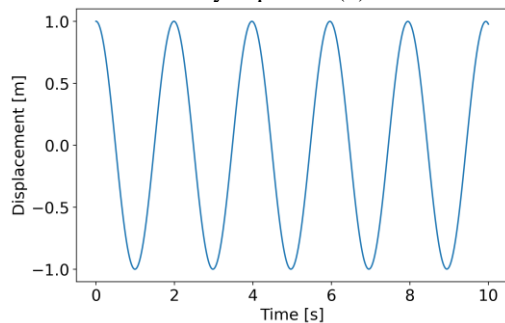


Fig. 2. The trajectory for an oscillating system described by Equation (2), with the parameters: mass  $m = 1$ , and stiffness  $k = 10$

By analysing a system with known parameters, its energy can be determined. When analysing non-linear phenomena, observing energy changes provides a more comprehensive understanding of the system's behaviour. The energy of a system encompasses various forms, including kinetic energy, potential energy, thermal energy, or chemical energy. This makes it a versatile descriptor that takes into account the various aspects of machine operation. Changes in the energy of a system can indicate changes in the efficiency of the machine. For example, a decrease in kinetic energy may indicate a decrease in machine efficiency related to wear and tear. Therefore, the following discussion focusses on the displacement of the system and its kinetic energy described by the equation.

$$E = \frac{1}{2} m \dot{x}^2. \quad (4)$$

And the potential energy.

$$U = \frac{1}{2} k x^2 \quad (5)$$

Figure 3 shows the evolution of potential, kinetic, and total energy for an oscillating system with one degree of freedom, characterised by the parameters: mass  $m=1$  and stiffness  $k=10$ . The system maintains a constant total energy, while the entropy of dispersion oscillates around the value of 2.4.

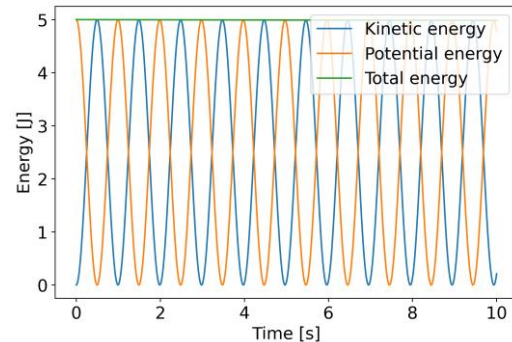


Fig. 3. The waveforms of potential, kinetic, and total energy for an oscillating system described by Equation (2), with the parameters: mass  $m = 1$  and stiffness  $k = 10$

For such a system, it is possible to analyse the smallest window width that can be used to obtain a repeatable DisEn value for vibration signals. The signal is harmonic, which makes it possible to neglect the influence of changes in amplitude, frequency, and noise values on the minimum measurement window length. Figures 4-7 show the dispersion entropy values with a sliding window as a function of the window length:  $\frac{1}{2} T$ ,  $T$ ,  $2T$ , and  $3T$  of the oscillation period of the system described by Equation (2). The vertical dashed lines mark the end of the measurement window, and in their place, the value of DisEn for the window is plotted.

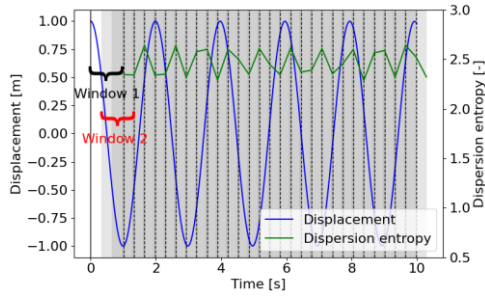


Fig. 4. DisEn value calculated for the displacement of an oscillating system described by Equation (2), with the parameters: mass  $m = 1$  and stiffness  $k = 10$ , with a window length of  $\frac{1}{2}$  the oscillation period:  $\text{win} = \frac{1}{2}T$

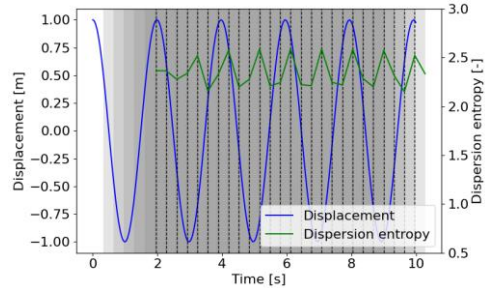


Fig. 5. DisEn value calculated for the displacement of an oscillating system described by Equation (2), with parameters: mass  $m = 1$  and stiffness  $k = 10$ , with a window length equal to the oscillation period:  $\text{win} = T$

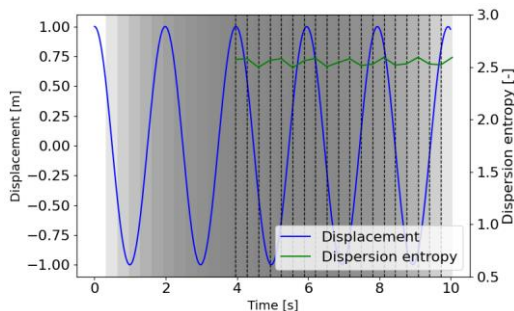


Fig. 6. DisEn value calculated for the displacement of an oscillating system described by Equation (2), with the parameters: mass  $m = 1$  and stiffness  $k = 10$ , with a window length equal to the oscillation period,  $\text{win} = 2T$

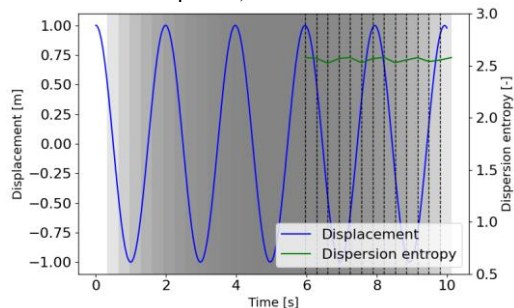


Fig. 7. DisEn value calculated for the displacement of an oscillating system described by Equation (2), with the parameters: mass  $m = 1$  and stiffness  $k = 10$ , with a window length equal to the oscillation period,  $\text{win} = 3T$

Figure 8 shows the dispersion results of the entropy for different time windows. On the x-axis is the window length, while on the y-axis is the value

of the entropy of dispersion. Each box corresponds to a different window length, as indicated by  $\frac{1}{2}T$ ,  $T$ ,  $2T$ , and  $3T$ , where  $T$  is the oscillation period of the analysed system. The dashed lines indicate the median entropy value for each window, and their lengths indicate the average entropy value in that window. In addition, the mean value is plotted on the graph.

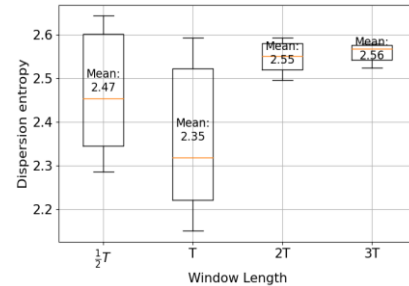


Fig. 8. DisEn values calculated for the displacement of an oscillating system described by Equation (2), with the parameters: mass  $m = 1$  and stiffness  $k = 10$ , with a window length equal to the period of oscillation,  $\text{win} = \frac{1}{2}T$ ,  $T$ ,  $2T$  and  $3T$

For free oscillations, DisEn needs at least a window of two oscillation periods. For a shorter window, the oscillations are about 10% of the DisEn value. It should be noted that for a window of less than 2 oscillations, the maximum values of DisEn have maximum values similar to those obtained with a longer measurement window. The maximum value can therefore be taken into account when a longer window is not possible and improve the rate of change detection in a system whose behaviour can be approximately described by equation (2).

### 2.2 Linear damping

Viscoelastic damping is a phenomenon that occurs in various mechanical and material systems, involving the conversion of the mechanical energy of vibration or motion into heat due to internal friction, which is characteristic of viscoelastic materials. This phenomenon is crucial in the context of engineering and material sciences, as it allows the control and reduction of vibration amplitudes in machines and structures, resulting in longer life and reliability. The mechanism of viscoelastic damping is based on the properties of viscous materials that, during deformation, exhibit resistance that depends on the speed of deformation. The effectiveness of viscous damping in a given material or system depends on several factors, including vibration frequency, temperature, and the physicochemical properties of the material.

In practice, viscous damping is used in a wide range of applications, from building structures to car components (e.g. shock absorbers) to advanced aerospace engineering systems. The use of damping materials and components makes it possible to effectively reduce vibrations and noise. The equation of motion with viscous damping is as follows.



$$m\ddot{x} + c\dot{x} + kx = 0, \quad (6)$$

where  $m$  is the mass,  $c$  is the damping coefficient and  $k$  is the stiffness coefficient. The solution to this equation can be written in the following form

$$x(t) = Ae^{-ht} \cos(\lambda t + \Phi) \quad (7)$$

where  $\lambda$  - vibration type parameter,  $\lambda^2 = \omega^2 - h^2$  an energy

$$E = \frac{1}{2} A^2 (e^{-ht})^2 (\cos(\lambda t + \Phi)^2 h^2 m + 2h\lambda m \cos(\lambda t + \Phi) \sin(\lambda t + \Phi) + \sin(\lambda t + \Phi)^2 \lambda^2 m + k \cos(\lambda t + \Phi)^2) \quad (8)$$

Figure 9 shows the unraveling of equation (7) for the parameters:  $m = 1$  kg,  $c = 0.3$  N\*s/m,  $k = 10$  N/m. Figure 10 shows the waveform of potential, kinetic, and total energy for an oscillating system with a degree of freedom for the parameters: mass  $m = 1$  kg,  $c = 0.3$  N\*s/m,  $k = 10$  N/m.

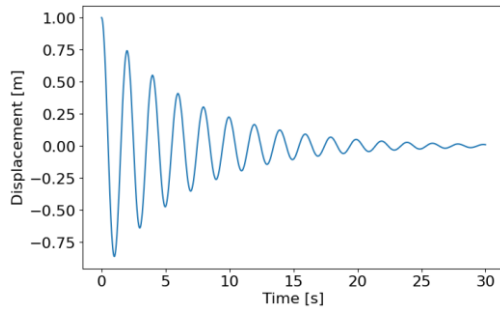


Fig. 9. The trajectory for the system described by Equation (5), with the parameters: mass  $m = 1$  kg,  $c = 0.3$  N\*s/m,  $k = 10$  N/m

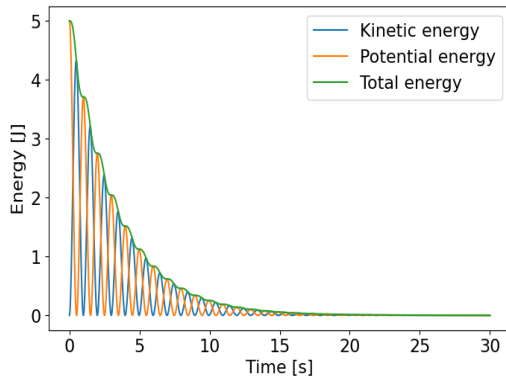


Fig. 10. Potential, kinetic, and total energy waveforms for the system described by Equation (5): mass  $m = 1$  kg,  $c = 0.3$  N\*s/m,  $k = 10$  N/m

Figures 11-14 show the dispersion entropy values with a sliding window as a function of the window length:  $\frac{1}{2}T$ ,  $T$ ,  $2T$ , and  $3T$  of the oscillation period of the system described by Equation (5).

Figure 15 shows the results of the entropy dispersion analysis for different time window lengths.

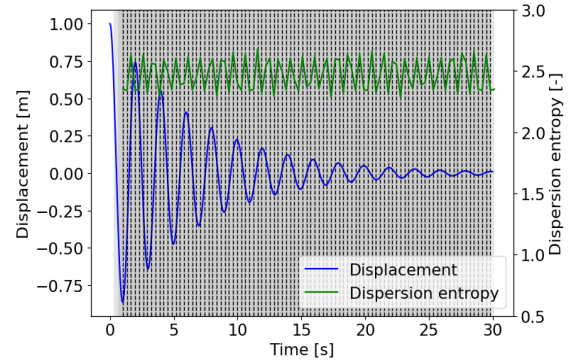


Fig. 11. DisEn value calculated for the displacement of the system described by Equation (6): mass  $m = 1$  kg,  $c = 0.3$  N\*s/m,  $k = 10$  N/m, with a window length equal to the period of oscillation,  $\text{win} = \frac{1}{2}T$

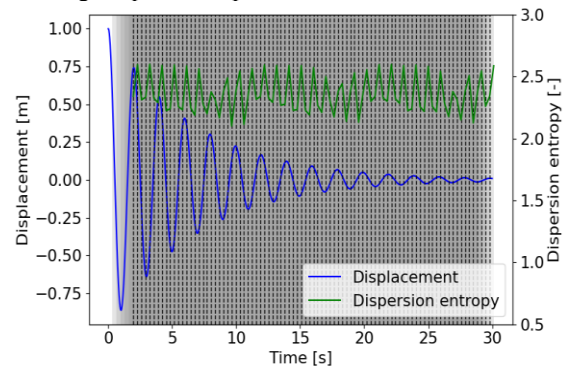


Fig. 12. DisEn value calculated for the displacement of the system described by Equation (6): mass  $m = 1$  kg,  $c = 0.3$  N\*s/m,  $k = 10$  N/m, with a window length equal to the period of oscillation,  $\text{win} = T$

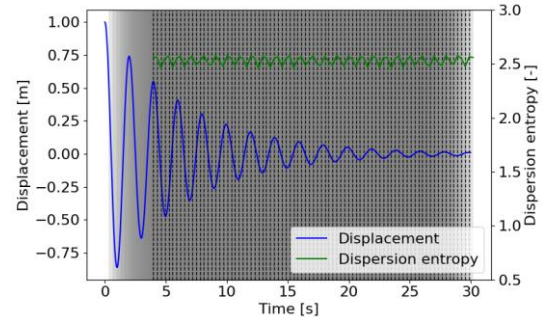


Fig. 13. DisEn value calculated for the displacement of the system described by Equation (6): mass  $m = 1$  kg,  $c = 0.3$  N\*s/m,  $k = 10$  N/m, with window length equal to two oscillation periods,  $\text{win} = 2T$

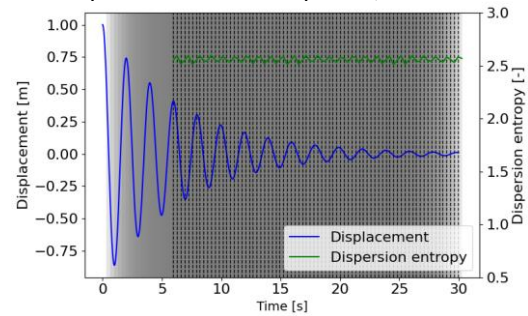


Fig. 14. DisEn value calculated for the displacement of the system described by Equation (6): mass  $m = 1$  kg,  $c = 0.3$  N\*s/m,  $k = 10$  N/m, with a window length equal to 3 oscillation periods,  $\text{win} = 3T$

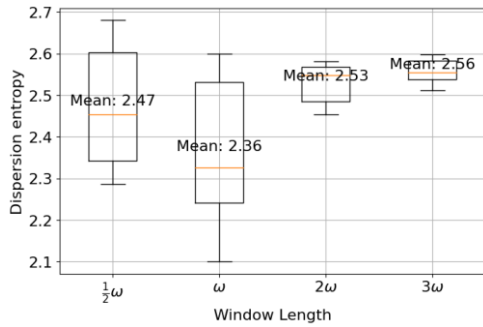


Fig. 15. DisEn values calculated for the displacement of the system described by Equation (6): mass  $m = 1 \text{ kg}$ ,  $c = 0.3 \text{ N*s/m}$ ,  $k = 10 \text{ N/m}$ , with a window length equal to the period of oscillation,  $\text{win} = \frac{1}{2}T, 1T, 2T$  and  $3T$

For free oscillations with linear damping, DisEn needs at least a window width of two oscillation periods. For a shorter window, the oscillations are about 10% of the DisEn value. As before, it can be seen that in the case of a window of less than 2 oscillations, the maximum values of DisEn have values similar to those obtained with a longer measurement window. The lack of sensitivity of the DisEn value to a change in the amplitude value is consistent with the results of the amplitude step studies from the work [20]. This should be taken into account in the application of DisEn for machine diagnostics. As will be shown later, the resistance to changes in amplitude can be used to assess the hydrodynamic stability as a result of the shape of the signal that excludes its amplitude.

### 2.3 Vibration with nonlinear damping

Attenuation can be of nonlinear form, which is written using the equation.

$$\ddot{x} + kx + 2h\dot{x} - b\dot{x}^3 = 0, \quad (9)$$

for:  $k, 2h, b > 0$

Equation (9), derived from the literature [18], involves parameters such as  $\beta$  (related to the damping coefficient) and  $k$  (the stiffness coefficient), with  $x$  representing displacement. This equation serves to characterise the behaviour of a nonlinear object and can simulate the damping that occurs in sliding bearings. The system's stability was assessed in the Lyapunov sense to analyse its behaviour as described by Equation (9). Numerical experiments were carried out to evaluate the potential application of the methods in the diagnosis of the hydrodynamic state of a sliding bearing. The study aimed to compare the behaviour of the values of the analysed methods in the context of the energy of the system, based on the principles of Newtonian mechanics. An increase in energy is observed when perturbations occur that lead to destabilisation of the system. Due to the cumbersome or impossible determination of the energy for complex real objects, the study was carried out on a simulated object.

The system (8) has three singularities  $(0,0)$ ,  $(-\sqrt{\frac{k}{2h}}, 0)$ ,  $(\sqrt{\frac{k}{2h}}, 0)$ . The first of these states is stable,

while the other two are unstable. Figure 16 shows a plot of the phase trajectories, highlighting the singularities, and illustrating all possible states of the system. The system exhibits instability that either seeks to increase displacement and velocity (quadrant I) or decreases displacement and velocity (quadrant III). Negative energy occurs when displacement and acceleration exceed velocity. Changing this sign can pose challenges in determining DisEn. Therefore, the system was examined by altering the parameter  $\beta$  associated with the damping ratio. Figure 17 presents the phase trajectories for the vibration of systems described by the given equation (9), illustrating the behavior of the system for different values of the parameter  $\beta$  in the range from 0.24 to 0.3.

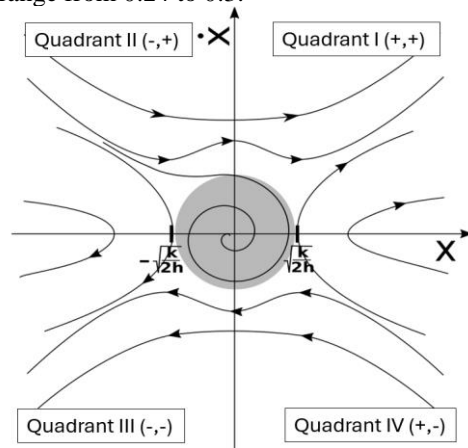


Fig. 16. Phase diagram for the system described by Equation (9)

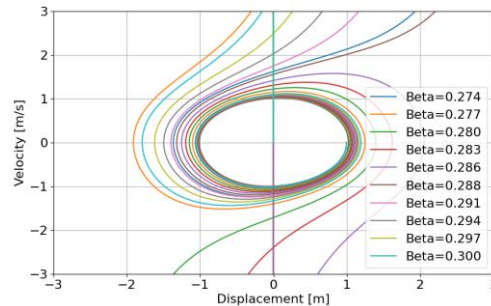


Fig. 17. Phase trajectories for vibration of systems described by Equation (9);  $k = 1, 2h = 0.2, \beta = 0.24 - 0.3, m = 1$

To analyse the value of DisEn in nonlinear damping, two examples were considered for the first  $\beta = 0.2739, 2h = 0.2, k = 1, m = 1$ . Figure 18 shows the displacement of this system; after 17 seconds, the value of the displacement increases rapidly.

Figure 19 shows the energy values for the system described by Equation (9) for the coefficients:  $\beta = 0.2739, 2h = 0.2, k = 1, m = 1$ . After 11 seconds, an increase in total energy is already visible, while after 17 seconds the increase is seen to spike. Figure 20 shows a phase trajectory graph showing the escape of the system from the stable point as velocity and acceleration increase. Figure 21 shows the variation of the DisEn value for a duration equal to two periods of oscillation. The fluctuations in value are

analogous to those observed in simpler systems. DisEn does not respond to a sudden change in displacement value.

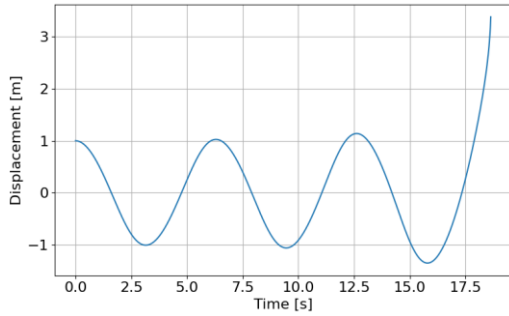


Fig. 18. Displacement of systems described by Equation (9);  $k = 1$ ,  $2h = 0.2$ ,  $\beta = 0.2739$ ,  $m = 1$

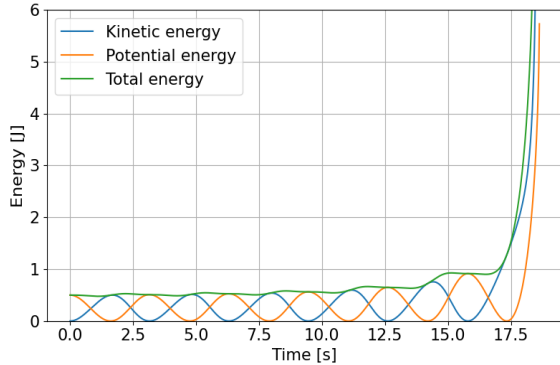


Fig. 19. Energy of systems described by Equation (9);  $k = 1$ ,  $2h = 0.2$ ,  $\beta = 0.2739$ ,  $m = 1$

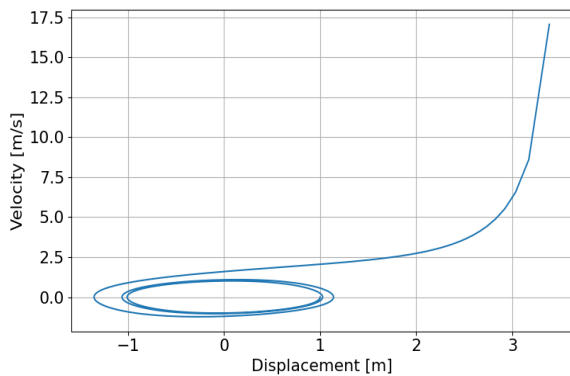


Fig. 20. Phase trajectories for the vibration of systems described by Equation (9);  $k = 1$ ,  $2h = 0.2$ ,  $\beta = 0.2739$ ,  $m = 1$

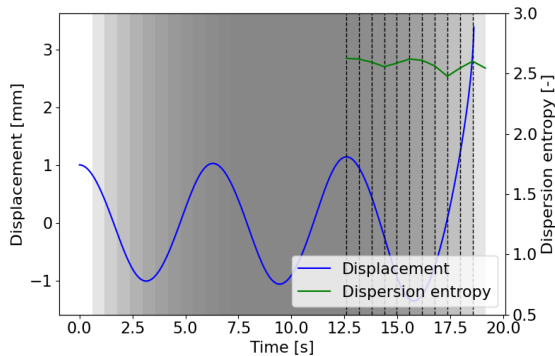


Fig. 21. DisEn for vibration of systems described by Equation (9);  $k = 1$ ,  $2h = 0.2$ ,  $\beta = 0.2739$ ,  $m = 1$ ; with window length equal to 2 periods of vibration,  $\text{win} = 2T$

Figure 22 shows analogously to the example shown above the displacement values for the system described by equation (9) for the coefficients:  $\beta = 0.28$ ,  $2h = 0.2$ ,  $k = 1$ ,  $m = 1$ . The system differs only in the beta value of the parameter by 0.71. However, this results in completely different system behaviour typical of chaotic systems, i.e. systems in which small changes in the input parameters cause significant changes in the system output. After 12 seconds, an increase in displacement can already be seen, while after 13 seconds there is a spike in the value of displacement. Figure 23 shows a graph of energy at 8 and 10 seconds showing an increase in energy, while at 14 it is abrupt. Figure 24 shows a phase trajectory graph showing the escape of the system from the stable point as the velocity and acceleration increase. Figure 25 shows the change in DisEn for a duration equal to 2 periods of oscillation. These changes are consistent with previous models.

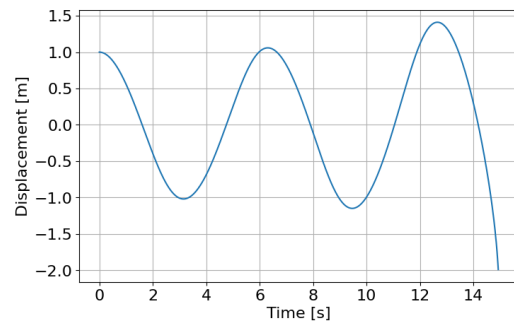


Fig. 22. Displacement of systems described by Equation (9);  $2h = 0.2$ ,  $\beta = 0.28$ ,  $k = 1$ ,  $m = 1$

### 3. EXPERIMENTAL BENCH TESTS

To perform the analysis of the actual signal, an experiment was designed and carried out on the laboratory bench shown in Figure 27. The bench setup includes a speed-controlled electric motor connected to a shaft through a coupling. The shaft is supported by rolling bearings at both ends, with the plain bearing under test positioned in the centre. Two eddy current sensors are mounted on the test bearing. The bearing utilised in this setup

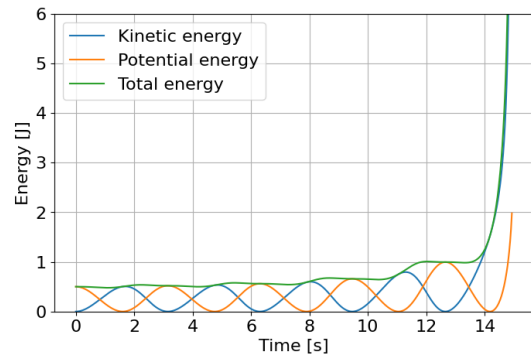


Fig. 23. Energy of systems described by Equation (9);  $2h = 0.2$ ,  $\beta = 0.28$ ,  $k = 1$ ,  $m = 1$



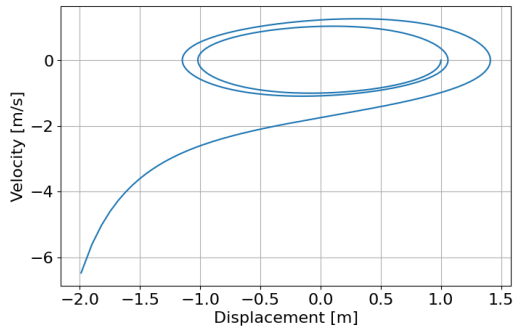


Fig. 24. Phase trajectories for vibration of systems described by Equation (9);  $2h = 0.2$ ,  $\beta = 0.28$ ,  $k = 1$ ,  $m = 1$

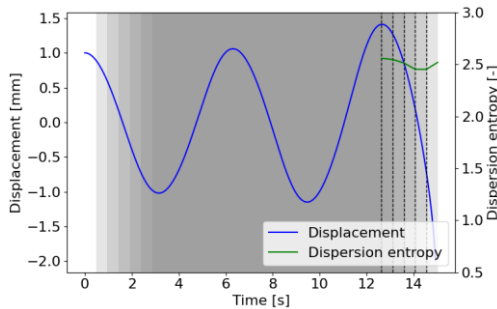


Fig. 25. DisEn for vibration of systems described by Equation (9);  $2h = 0.2$ ,  $\beta = 0.2739$ ,  $k = 1$ ,  $m = 1$ ; with window length equal to 2 periods of vibration,  $win = 2T$

is a water-lubricated multi-shaft plain bearing. This bearing, also known as a cutlass bearing, is a type of marine bearing used to support rotating shafts on boats and ships. It is a commercial bearing designed to fit a 20mm diameter shaft. Eddy current sensors are used as distance sensors, allowing direct tracking of the distance on the x and y axes, as shown in Figure 26. A laser tachometer measures the shaft speed. The lubrication system works on the principle of a closed water circuit as a lubricant, with water entering the bearing and draining from there. Measurement data, such as the signal from the tachometer and the x- and y-axis displacements from the eddy current sensors, are recorded using a measuring card with a sampling frequency of 4200 Hz and a 16-bit analogue-to-digital converter.

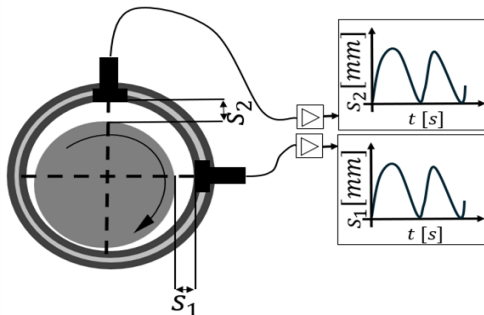


Fig. 26. Vibration monitoring system of cutlass-bearing nodes

The signal analysed in eddy current sensor measurement systems is disturbed by inhomogeneities in the shape and physical properties of the shaft surface. In the literature, the disturbance associated with eddy current measurements is called

‘runout’. A distinction can be made between mechanical and electrical run-out. Mechanical failure is related to imperfections in the shape of the shaft under test, such as roughness, ripples, the presence of scratches, dents, or other deformations. Electrical discharge is related to magnetic inhomogeneities on the surface of the shaft under test. The lack of consistent magnetic surface features is the result of mechanical machining processes (e.g., turning). This machining creates residual stresses, which are the direct cause of the observed variation in the electrical run-out of the shaft surface. Due to the interference mentioned, the signal is filtered using a Butterworth bandpass filter. In the experiment, the analysis was carried out by observing the frequency corresponding to the rotation of the rotor in the band from 0.3 to 2.4 of the rotational frequency. Diagnostic information on the operation of the stability of the plain bearing can be identified on the rotational trajectory.

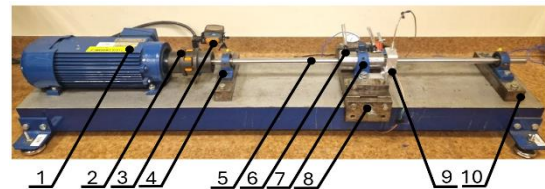


Fig. 27. Test stand: 1 - motor with speed control system, 2 - clutch, 3 - non-contact digital laser tachometer, 4, 10 - rolling bearings, 5 - shaft, 6 - journal bearing, 7 - lubricant supply and discharge valves, 8 - bearing loading system, 9 - eddy current sensors

The experiment carried out makes it possible to observe the effect of the length of the displaced DisEntr window on mechanical systems to detect the loss of stability of rotating machinery. The displacement signal for the x-axis was analysed (Figure 28). The unstable and stable operation of the cutless plain bearing was recorded at a rotational speed of 4300 rpm. Figure 29 shows the variation of the DisEn value for a window of one revolution length (T). Figure 30 shows the fluctuation of the DisEn value for a window of two revolutions (2T). When comparing the two cases, it can be seen that extending the sliding window produces more stable results, which is consistent with observations made on simulated signals.

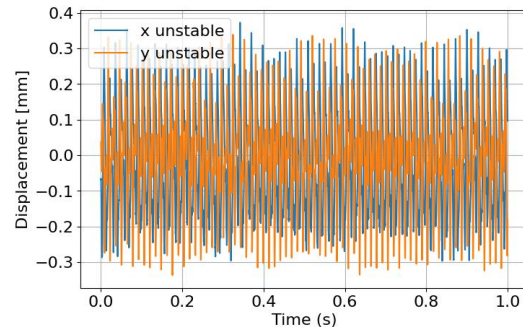


Fig. 28. Recorded displacement signal for the x and y axes during unstable operation of a plain bearing

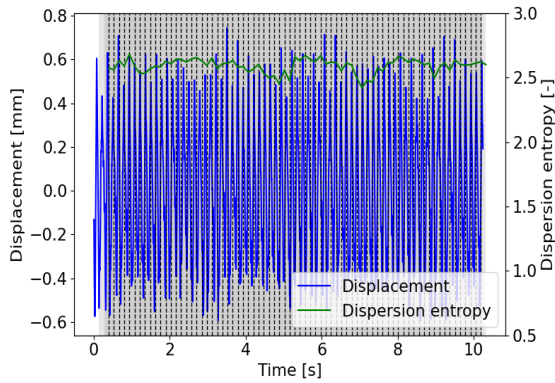


Fig. 29. Dispersion entropy for unstable operation for a window length that contains one full rotation of the rotor

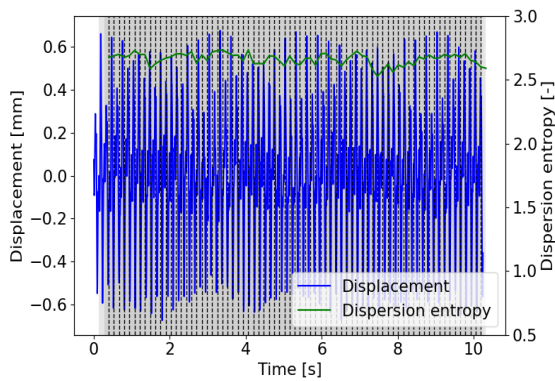


Fig. 30. Dispersion entropy for unstable operation for a window length containing two full rotations of the rotor

The second experiment concerned the analysis of stable operation. The signal was recorded for the same speed and load, and stabilisation was achieved by increasing the lubricant density. The displacement signal for the x-axis was analysed (Figure 31). Figure 32 shows the variation of the DisEn value for a window of one rotation length ( $T$ ). Figure 33 shows the variation of the DisEn value for a window of two revolutions ( $2T$ ). When comparing the two cases, it can be seen that extending the sliding window produces more stable results, which is consistent with observations made on simulated signals.

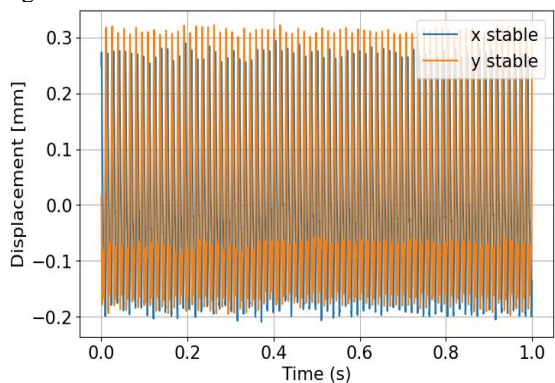


Fig. 31. Recorded displacement signal for the x and y axes during stable operation of a cutless plain bearing

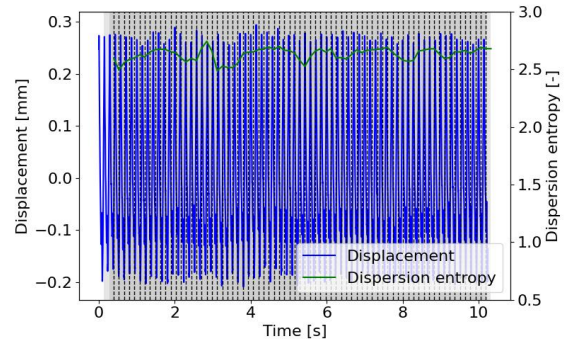


Fig. 32. Dispersion entropy for stable operation for a window length that contains one full rotation of the rotor

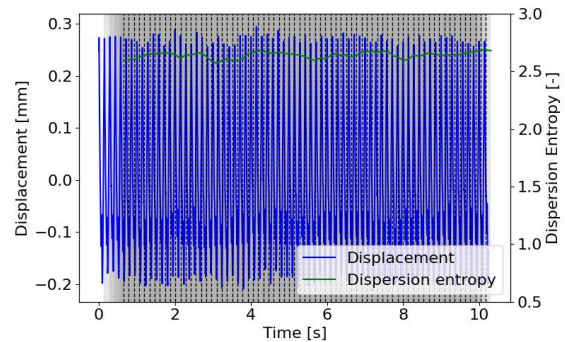


Fig. 33. Dispersion entropy for stable operation for a window length containing two full rotations of the rotor

Figure 34 shows a box plot of the obtained DisEn values for a length she short-circuits two full rotations. A significant decrease in the DisEn values can be observed for the y-axis. However, the changes in the x-axis do not allow a clear assessment of the change in DisEn for unstable and stable operation of the tested plain bearing.

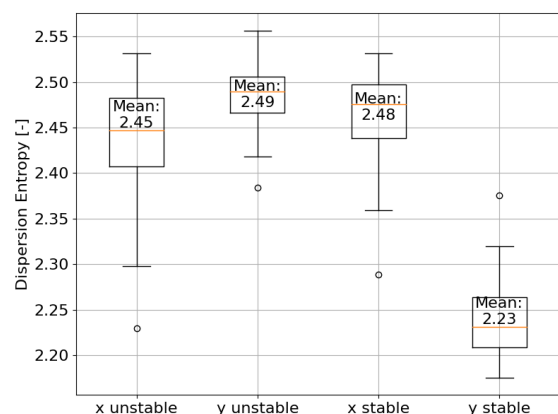


Fig. 34. Dispersion entropy for unstable and stable operation over a window length containing two full rotations

This paper focuses on the influence of the DisEn window length on the application of this method to rotating machinery. On the basis of simulated signals, the need for a window length of at least 2 vibration periods was noted. This conclusion is consistent with methods for evaluating plain

bearings, where at least two rotations are evaluated to assess the rotational trajectory of the shaft relative to the bearing pan. Figure 35 shows the difference in the DisEn values for the x and y signals for stable and unstable operation and its variation with window length. It can be seen that to distinguish between the signals, the length of the window needs to be extended so that it is at least 1 revolution, while there is no significant change in these values after 2 revolutions.

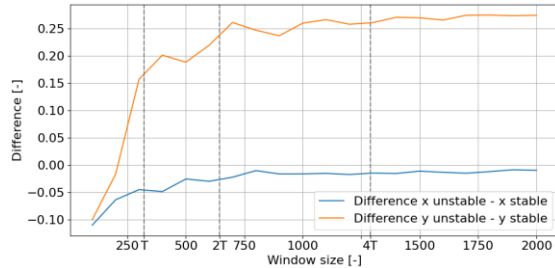


Fig. 35. Difference between unstable and stable values due to the change in window length from 100 to 2000 samples with marked window length equal to 1, 2 and 4 shaft rotations

#### 4. SUMMARY AND CONCLUSIONS

This article explores the application of dispersion entropy (DisEn) with a sliding window to assess the stability of machine operations. Research focusses on determining the minimum window length that ensures stable diagnostic results, which is crucial to reducing computational demands and accelerating response times. The study covers simple mechanical systems, nonlinear systems, and real signals from hydrodynamic bearings, to improve diagnostic accuracy and efficiency.

Initially, simulation studies were conducted on simple mechanical systems, such as single-degree-of-freedom oscillators, analysing natural and linearly damped vibrations. The findings indicated that, for free oscillations, the DisEn value required a window of at least two oscillation periods to achieve repeatable results. Windows shorter than two periods resulted in DisEn value oscillations of about 10%, highlighting the need for longer measurement windows.

The research was then extended to systems with nonlinear damping, such as sliding bearings, using equations that describe nonlinear damping. Numerical experiments demonstrated that changes in damping parameters significantly affected the system behaviour, as evidenced by phase trajectories and total energy variations. DisEn values for systems with nonlinear damping also required windows of at least two oscillation periods to maintain stability.

In the second part of the study, experimental investigations were performed on real signals from hydrodynamic bearings. A laboratory setup was designed that included a speed-controlled electric motor, a rolling bearing, and a test bearing equipped with eddy current sensors. The analysis of displacement signals showed that during unstable

bearing operation, the DisEn value varied significantly with window length. Longer sliding windows (at least two full shaft rotations) produced more stable results, consistent with simulation observations. For stable bearing operation, while the changes in DisEn values were less pronounced, the benefits of longer windows remained evident.

The study concludes that the minimum window length to obtain stable DisEn values is at least two oscillation periods. Shorter windows lead to unstable results, complicating accurate diagnostics. DisEn proves to be an effective tool for monitoring vibrational signal instability in machine diagnostics, allowing the rapid detection of subtle irregularities. Although shorter measurement windows can expedite the diagnostic process, they do so at the expense of the stability of the result. Longer windows ensure stability and accuracy, crucial for practical applications.

The experimental results validate the simulation findings, reinforcing the reliability of the conclusions and suggesting further research on optimising diagnostic parameters for various types of machinery. Future research should focus on the continued miniaturisation of measurement devices, integration with the Internet of Things (IoT), and the development of intelligent algorithms capable of predictive maintenance.

In summary, this article makes a significant contribution to the development of diagnostic methods based on dispersion entropy. Findings can improve the efficiency and precision of machine diagnostics, directly affecting the safety and reliability of machine operations.

**Source of funding:** *This research received no external funding.*

**Author contributions:** *research concept and design, J.B.; Collection and/or assembly of data, J.B., Ł.B.; Data analysis and interpretation, J.B., Ł.B.; Writing the article, J.B., Ł.B.; Critical revision of the article, J.B., Ł.B.; Final approval of the article, J.B., Ł.B.*

**Declaration of competing interest:** *The authors declare that they have no known competing financial interests or personal relationships that could have appeared to influence the work reported in this paper.*

#### REFERENCES

1. Mobley RK. Benefits of predictive maintenance. *An Introduction to Predictive Maintenance*. 2002;60–73. <https://doi.org/10.1016/B978-075067531-4/50004-X>.
2. Tavner PJ. Review of condition monitoring of rotating electrical machines. *IET Electric Power Applications*. 2008;2(4):215. <https://doi.org/10.1049/iet-epa:20070280>.
3. Mourtzis D, Vlachou E, Milas N. Industrial Big Data as a Result of IoT Adoption in Manufacturing.



- Procedia CIRP. 2016; 55: 290–5.  
<https://doi.org/10.1016/j.procir.2016.07.038>.
4. Pincus SM. Approximate entropy as a measure of system complexity. Proceedings of the National Academy of Sciences. 1991;88(6):2297–301.  
<https://doi.org/10.1073/pnas.88.6.2297>.
  5. Lee J, Lapira E, Bagheri B, Kao H an. Recent advances and trends in predictive manufacturing systems in big data environment. Manufacturing Letters. 2013; 1(1): 38–41.  
<https://doi.org/10.1016/j.mfglet.2013.09.005>.
  6. Ziółkowski P, Drosińska-Komor M, Gluch J, Breńkacz Ł. Review of methods for diagnosing the degradation process in power units cooperating with renewable energy sources using artificial intelligence. Energies. 2023;16(17):6107.  
<https://doi.org/10.3390/en16176107>.
  7. García Márquez FP, Tobias AM, Pinar Pérez JM, Papaalias M. Condition monitoring of wind turbines: Techniques and methods. Renewable Energy. 2012; 46:169–78.  
<https://doi.org/10.1016/j.renene.2012.03.003>.
  8. Breńkacz Ł, Żywica G. Comparison of experimentally and numerically determined dynamic coefficients of the hydrodynamic slide bearings operating in the nonlinear rotating system. In Proceedings of the Volume 7A: Structures and Dynamics; American Society of Mechanical Engineers. 2017;7A:1–12.
  9. Żywica G, Breńkacz Ł, Bagiński P. Interactions in the rotor-bearings-support structure system of the multi-stage ORC microturbine. Journal of Vibration Engineering & Technologies 2018;6(5):369–77.  
<https://doi.org/10.1007/s42417-018-0051-2>.
  10. Randall RB. Vibration-based condition monitoring: industrial, Automotive and Aerospace Applications. Wiley. 2011.
  11. Tandon N, Choudhury A. A review of vibration and acoustic measurement methods for the detection of defects in rolling element bearings. Tribology International 1999;32(8):469–80.  
[https://doi.org/10.1016/S0301-679X\(99\)00077-8](https://doi.org/10.1016/S0301-679X(99)00077-8).
  12. Breńkacz Ł. The experimental identification of the dynamic coefficients of two hydrodynamic journal bearings operating at constant rotational speed and under nonlinear conditions. Polish Maritime Research 2017;24(4):108–15.  
<https://doi.org/10.1515/pomr-2017-0142>.
  13. Breńkacz Ł. the experimental identification of the dynamic coefficients of two hydrodynamic journal bearings operating at constant rotational speed and under nonlinear conditions. Polish Marit. Res. 2017;24:108–115.  
<https://doi:10.1515/pomr-2017-0142>.
  14. Breńkacz Ł, Żywica G. The sensitivity analysis of the method for identification of bearing dynamic coefficients. dynamical systems. Modelling. 2015; Springer International Publishing 2016;81–96.
  15. Breńkacz Ł. Bearing dynamic coefficients in rotordynamics. 1st ed. Wiley .2021. Antoniadou I, Manson G, Staszewski WJ, Barszcz T, Worden K. A time–frequency analysis approach for condition monitoring of a wind turbine gearbox under varying load conditions. Mechanical Systems and Signal Processing. 2015;64–65:188–216.  
<https://doi.org/10.1016/j.ymsp.2015.03.003>.
  16. Antoniadou I, Manson G, Staszewski WJ, Barszcz T, Worden K. A time–frequency analysis approach for condition monitoring of a wind turbine gearbox under varying load conditions. Mech Syst Signal Process. 2015;64–65:188–216.  
<https://doi.org/10.1016/j.ymsp.2015.03.003>.
  17. Lu C, Wang ZY, Qin WL, Ma J. Fault diagnosis of rotary machinery components using a stacked denoising autoencoder-based health state identification. Signal Processing. 2017;130:377–88.  
<https://doi.org/10.1016/j.sigpro.2016.07.028>.
  18. Blaut J, Breńkacz Ł. Application of the Teager-Kaiser energy operator in diagnostics of a hydrodynamic bearing. Eksploatacja i Niezawodność – Maintenance and Reliability. 2020;22(4):757–65.  
<https://doi.org/10.17531/ein.2020.4.20>.
  19. Rostaghi M, Azami H. Dispersion entropy: A measure for time-series analysis. IEEE Signal Processing Letters. 2016;23(5):610–4.  
<https://doi.org/10.1109/LSP.2016.2542881>.
  20. Rostaghi M, Ashory MR, Azami H. Application of dispersion entropy to status characterization of rotary machines. Journal of Sound and Vibration. 2019; 438:291–308.  
<https://doi.org/10.1016/j.jsv.2018.08.025>.
  21. Case Western Reserve University Bearing Data Center. Bearing fault data for condition monitoring of bearings. Accessed. [09,2024].  
<https://engineering.case.edu/bearingdatacenter>.
  22. Mobley RK. Benefits of predictive maintenance. in an introduction to predictive maintenance. Elsevier. 2002;2:60–73.
  23. Bandt C, Pompe B. Permutation Entropy: A natural complexity measure for time series. Physical Review Letters. 2002;88(17):174102.  
<https://doi.org/10.1103/PhysRevLett.88.174102>.
  24. Sandoval D, Leturiondo U, Vidal Y, Pozo F. Entropy indicators: An approach for low-speed bearing diagnosis. Sensors. 2021;21(3):849.  
<https://doi.org/10.3390/s21030849>.



**Jędrzej BLAUT**

PhD (Engineering), AGH University of Science and Technology, Kraków.  
e-mail:[blaut@agh.edu.pl](mailto:blaut@agh.edu.pl)



**Łukasz BREŃKACZ** - PhD (Engineering), research associate at the Institute of Fluid Flow Machinery, Polish Academy of Sciences in Gdańsk, and research associate at the AGH University of Kraków; <http://brenkacz.com/>; e-mail: [lbrenkacz@imp.gda.pl](mailto:lbrenkacz@imp.gda.pl)